

Development of a yeast model system for interrogating the influence of beta-oxidation on mitochondrial cardiolipin turnover

Ivanov, Ana Maria

Undergraduate thesis / Završni rad

2023

Degree Grantor / Ustanova koja je dodijelila akademski / stručni stupanj: **University of Rijeka / Sveučilište u Rijeci**

Permanent link / Trajna poveznica: <https://um.nsk.hr/um:nbn:hr:193:786797>

Rights / Prava: [In copyright](#)/[Zaštićeno autorskim pravom.](#)

Download date / Datum preuzimanja: **2025-03-31**

Repository / Repozitorij:



[Repository of the University of Rijeka, Faculty of Biotechnology and Drug Development - BIOTECHRI Repository](#)



UNIVERSITY OF RIJEKA
DEPARTMENT OF BIOTECHNOLOGY
Undergraduate university programme
Biotechnology and drug research

Ana Maria Ivanov

**Development of a yeast model system for interrogating the influence
of beta-oxidation on mitochondrial cardiolipin turnover**

Rijeka, 2022.

Mentor: Christian A. Reynolds, PhD.

SVEUČILIŠTE U RIJECI
ODJEL ZA BIOTEHNOLOGIJU
Preddiplomski sveučilišni studij
Biotehnologija i istraživanje lijekova

Ana Maria Ivanov

**Razvoj modelnog Sistema kvasca za ispitivanje utjecaja beta-
oksidacije na promjenu mitohondrijskih kardiolipina**

Rijeka, 2022.

Mentor: doc.dr.sc. Christian A. Reynolds

Undergraduate final thesis was defended on September 19th, 2022.

In front of the Committee:

1. Associate Prof. Antonija Jurak Begonja
2. Prof. Anđelka Radojčić Badovinac
3. Assistant Prof. Christian Reynolds

This thesis has 31 pages, 12 figures and 18 citations

Abstract

Barth syndrome is a multi-system genetic disorder that affects the mitochondria. It is characterized by a wide range of conditions mostly affecting the heart and skeletal muscles. Symptoms include: cardiomyopathy, skeletal myopathy, neutropenia, increased urinary excretion of 3-methylglutaconic acid and weaker motor skills. What causes the disorder is the mutations in the tafazzin (TAZ) gene, which codes the tafazzin enzyme that, in healthy cells, is widely present in cardiac and skeletal muscles and takes part in the cardiolipin remodeling pathway. Cardiolipin is a phospholipid located in the mitochondrial inner membrane. Unlike other phospholipids, cardiolipin has a specific structure which allows it to interact with a variety of membrane proteins and complexes, giving the molecule important functions in proper mitochondrial energy metabolism. It undergoes a highly conserved and complex synthesis pathway, which is altered in patients with Barth syndrome. Since there exists a lack of understanding the importance and functions of cardiolipin synthesis, Barth syndrome is treated only symptomatically. With improved understanding of the molecular mechanism and importance of cardiolipin synthesis and remodeling, new treatment approaches for Barth syndrome can be evaluated. One such target may be beta-oxidation. Trimetazadine is a drug widely used for treating heart conditions, which inhibits beta-oxidation and in some previous research influences mitochondrial phospholipid turnover. However, the effect of trimetazadine on cardiolipin synthesis and turnover is unknown. We are curious to see whether the inhibition of beta-oxidation promotes mitochondrial phospholipid turnover and increases functional cardiolipin content in cells with TAZ deficiencies. *Saccharomyces cerevisiae* is a great model organism for studying Barth syndrome because all enzymatic steps in the cardiolipin synthesis and remodeling pathway are conserved from yeast to humans.

Sažetak

Barthov sindrom je multi-sistemska genetska poremećaj koji zahvaća mitohondrij. Karakteriziran je širokim rasponom stanja koja uglavnom zahvaćaju srce i skeletne mišiće. Simptomi uključuju: kardiomiopatiju, skeletnu miopatiju, neutropeniju, povećano izlučivanje 3-metilglutakonske kiseline i slabije motoričke sposobnosti. Poremećaj uzrokuju mutacije u tafazzin (TAZ) genu koji kodira enzim tafazzin koji je, u zdravim stanicama, velikim brojem prisutan u srcu i skeletnim mišićima te sudjeluje u putu remodeliranja kardiolipina. Kardiolipin je fosfolipid lociran u unutarnjoj membrani mitohondrija. Za razliku od drugih fosfolipida, kardiolipin ima specifičnu strukturu koja mu omogućava interakciju s brojnim membranskim proteinima i kompleksima, dajući molekuli važne funkcije u pravilnom mitohondrijskom metabolizmu. Podvrgava se visoko očuvanom i kompleksnom sintetskom putu, koji je promijenjen u pacijenata koji boluju od Barthovog sindroma. S obzirom na smanjeno razumijevanje važnosti i funkcije sinteze kardiolipina, Barthov sindrom se liječi simptomatski. Uz bolje razumijevanje molekularnog mehanizma i funkcije kardiolipinske sinteze i remodeliranja, mogu se procijeniti novi pristupi liječenju Barthovog sindroma. Jedna od meta u liječenju mogla bi biti beta-oksidacija. Trimetazidin je lijek široke primjene u liječenju srčanih oboljenja, koji inhibira beta-oksidaciju te u ranije provedenim istraživanjima utječe na promjenu mitohondrijskih fosfolipida. Unatoč tome, utjecaj trimetazidina na promjenu i sintezu kardiolipina je nepoznat. Zanima nas vidjeti promovira li inhibicija beta-oksidacije promjenu mitohondrijskih fosfolipida i povećanje funkcionalnog kardiolipina u stanicama s TAZ deficijencijama. *Saccharomyces cerevisiae* je odličan modelni organizam za proučavanje Barthovog sindroma zbog činjenice da su svi koraci sinteze i remodeliranja kardiolipina sačuvani od kvasca do čovjeka.

Contents:

| | |
|--|----|
| Introduction | 1 |
| Barth syndrome..... | 1 |
| Cardiolipin and cardiolipin remodeling..... | 2 |
| Trimetazadine and phospholipid turnover..... | 5 |
| <i>S. cerevisiae</i> as a model organism..... | 6 |
| Thesis objectives | 7 |
| Materials and methods | 8 |
| Protein alignment..... | 8 |
| <i>S. cerevisiae</i> cell lines..... | 8 |
| Growth conditions..... | 9 |
| Glucose deprived spotting assay..... | 9 |
| Fatty acid as sole carbon source spotting assay..... | 10 |
| Extraction of genomic DNA from yeast..... | 11 |
| PCR and gel electrophoresis..... | 11 |
| Yeast transformation..... | 14 |
| One step yeast transformation..... | 14 |
| Electroporation..... | 15 |
| Results | 16 |
| Discussion | 26 |
| Future goals and objectives | 28 |
| Conclusion | 29 |
| References | 30 |

Introduction

Barth syndrome

Barth syndrome is a rare genetic disorder first described in 1983. by Dr. Peter Barth. It is a recessive X-linked disease that affects one of the cells organelles - the mitochondria and is characterized by a wide spectrum of conditions including: cardiomyopathy (typically dilated cardiomyopathy) and ventricular arrhythmia; skeletal and muscle problems such as skeletal myopathy and growth delay; low to non-existent neutrophil count and highly increased urinary excretion of 3-methylglutaconic acid (3-MGCA)(1). Other health problems include pubertal growth delay, delayed motor milestones and recurrent bacterial infections due to neutropenia. Although the issue of largest impact are cardiac problems, Barth syndrome is a multi-system disorder. This makes it hard to diagnose given its wide spectrum of symptoms not all of which are always present in every patient(2). The disease is caused by loss of function mutations of the tafazzin (TAZ) gene, located at Xq28. The TAZ gene codes for the tafazzin enzyme, which is highly present in cardiac and skeletal muscle and is involved in remodeling the mitochondrial phospholipid cardiolipin(3). Given the fact that this disease is a genetic disorder, it is incurable, but it can be managed with heart failure medications and treatments(2). Although it is known that Barth syndrome as well as many other cardiac illnesses are associated with altered myocardial cardiolipin composition, none of the existing treatments target mitochondrial phospholipid homeostasis.

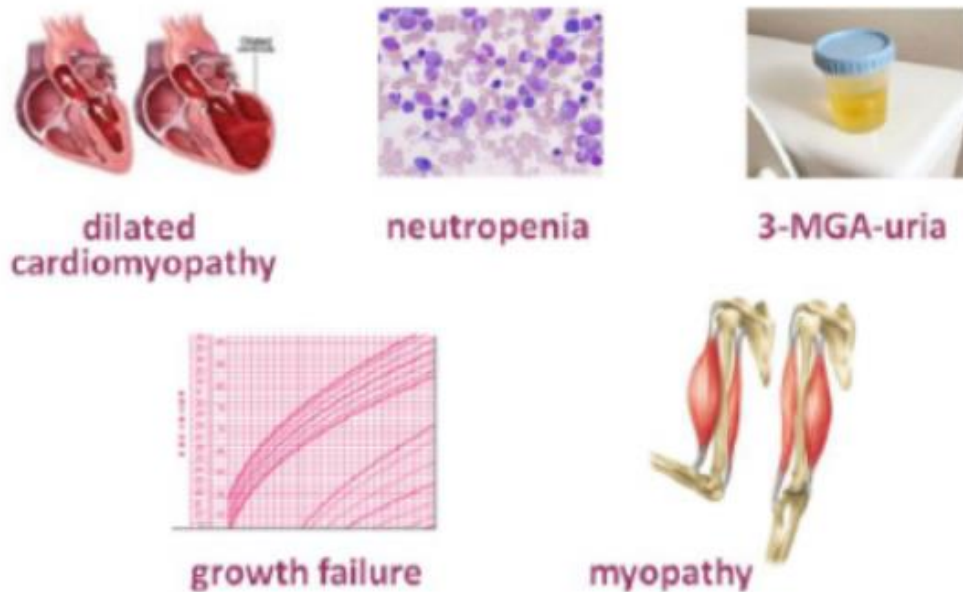


Figure 1 : Barth syndrome indications. Most common indications of Barth syndrome include dilated cardiomyopathy, neutropenia, skeletal myopathy, skeletal and muscle growth failure and presence of elevated 3-MGCA levels in urine. Taken from (4)

Cardiolipin and cardiolipin remodeling

Cardiolipin is a unique phospholipid located in the mitochondrial inner membrane. It constitutes about 15% of the total mitochondrial phospholipidome, making it an important part of proper mitochondrial functioning. It differs from other phospholipids in its structure – it has two phosphatidyl moieties, four acyl (fatty acid) chains and two negative charges. Because of its unique structure, it interacts with various mitochondrial proteins, such as respiratory complexes and the ADP/ATP carrier. The main functions of this phospholipid are stabilizing respiratory chain supercomplexes and promoting their interactions with the ADP/ATP carrier (4). Cardiolipin is also involved in many other cellular functions included in mitochondrial protein import, mitochondrial morphology, cell cycle regulation and apoptosis, which leads us to a conclusion that cardiolipin homeostasis is crucial for the normal

mitochondrial and cellular functioning (4). The synthesis of cardiolipin is unique, highly conserved and complex, as it has many precursors and genes coding specific enzymes involved.

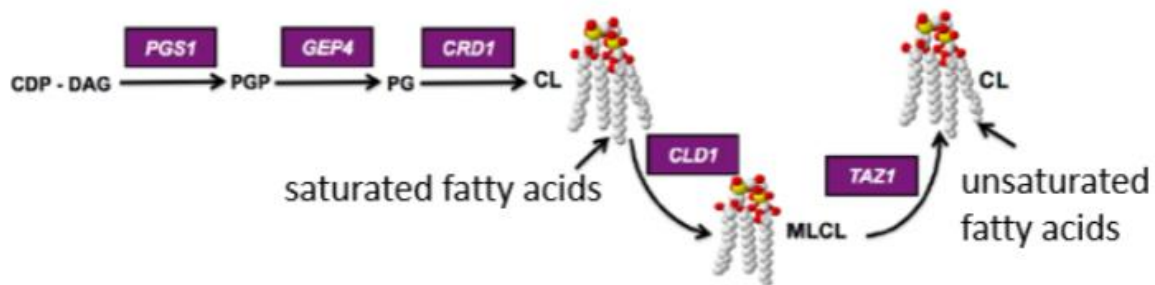


Figure 2 : Cardiolipin synthesis and remodeling in *S. cerevisiae*. Cardiolipin is synthesized at the inner membrane of the mitochondria from phosphatidic acid precursors that are imported from the endoplasmic reticulum into the mitochondria. The precursors react with cytidine triphosphate (CTP) to form cytidine diphosphate-diacylglycerol (CDP-DAG). Phosphatidylglycerol phosphate synthase (PGS1) catalyzes fusion between CDP-DAG and glycerol-phosphate that forms phosphatidylglycerol phosphate (PGP) which is then dephosphorylated (PG) by the mitochondrial phosphatidylglycerophosphatase (GEP4) (5). Then, cardiolipin synthase 1 (CRD1) turns the phosphatidylglycerol into cardiolipin by adding saturated fatty acids. This cardiolipin undergoes remodeling, with the first step being removing one fatty acid chain from the 4 chain *de novo* synthesized cardiolipin. This is catalyzed by mitochondrial cardiolipin-specific deacylase 1 (CLD1) that converts cardiolipin into monolysocardiolipin (MLCL), a three chain variant of cardiolipin. Finally, the enzyme tafazzin (an acetyltransferase) remodels MLCL into cardiolipin containing unsaturated fatty acids. Taken from (4)

Given the complex nature of cardiolipin synthesis, it was unclear whether Barth syndrome is caused by the loss of remodeled cardiolipin that contains predominantly unsaturated fatty acyl residues or by the accumulation of the monolyso cardiolipin (MLCL) intermediates that are missing one fatty acid residue. As shown in Figure 3, this was answered using *S. cerevisiae* as a model organism by Ye et. al. (4). They constructed a *cld1Δtaz1Δ* double mutant, which completely lacks cardiolipin remodeling. Like the *taz1Δ*, the *cld1Δtaz1Δ* double mutant contains cardiolipin with predominately saturated

fatty acyl residues; however, unlike the *taz1Δ* strain, the *clد1Δtaz1Δ* double mutant does not accumulate MLCL. Given that the *clد1Δtaz1Δ* double mutant does not display any mitochondrial or growth defects, the phenotypes associated with TAZ mutations likely arise from the accumulation of MLCL within the mitochondrial membrane. Accordingly, at least in yeast, newly synthesized unremodeled cardiolipin is sufficient for proper mitochondrial function.

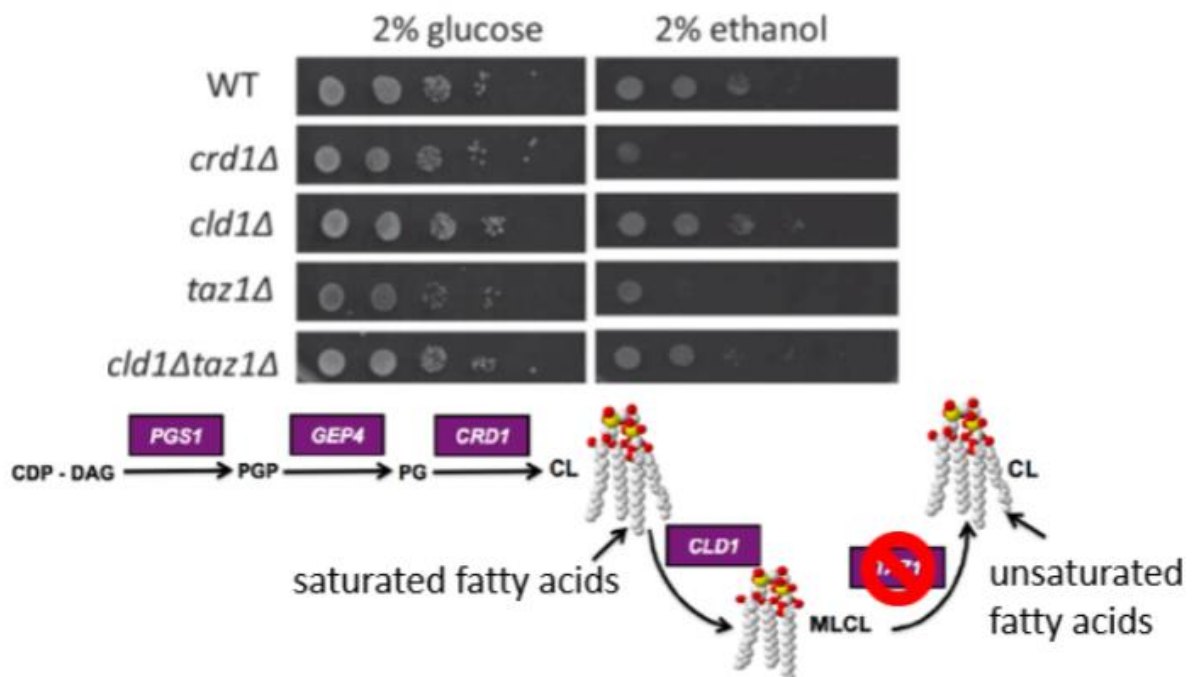


Figure 3: Deletion of CLD1 rescues growth in *taz1Δ* yeast mutant. WT, *crد1Δ*, *clد1Δ*, *taz1Δ* and *clد1Δtaz1Δ* yeast mutants were grown on two different carbon sources – 2% glucose and 2% ethanol. WT was used as a control as well as the 2% glucose media that uses as a growth comparison, given the fact that yeast cells use glucose as their main source of energy. Ethanol as a carbon source makes it harder for yeast to grow because they have to change their metabolism to heavily rely on the mitochondria, due to glycolysis being an unavailable metabolic pathway for energy gain. What is observed is that the absence of CRD1 and TAZ1 makes it almost impossible for cells to grow due to the lack of cardiolipin synthesis and remodeling. Absence of CLD1 still made it possible for cells grow, even in TAZ1 lacking yeast, which lead to the conclusion that Barth syndrome is not caused by unremodeled cardiolipin, but by accumulation of MLCL, since the lack of TAZ1 was rescued by CLD1 deletion. Taken from (4)

Trimetazadine and phospholipid turnover

Trimetazadine is an anti-ischemic compound widely used in the treatment of heart conditions, mainly coronary artery disease. Trimetazadine has shown to improve health conditions in patients suffering from angina and to be helpful during angioplasty and coronary artery bypass surgery due to its antiischemic activity (6). Its mechanism of action revolves around inhibiting beta-oxidation by disrupting the function of the mitochondrial 3-ketoacyl coenzyme A thiolase enzyme. This leads to an improvement of mitochondrial metabolism because of the myocardial fatty acid uptake and oxidation are inhibited while glucose oxidation is stimulated. The drug differs from other conventional drugs because it doesn't affect coronary flow, cardiac contractility, heart rate or blood pressure. Additionally, it can be combined with many other conventional therapies used for coronary artery disease or as a substitution therapy in patients who have an intolerance to conventional therapy (7). In addition to inhibiting beta-oxidation, treatment with trimetazadine causes changes to the mitochondrial phospholipome (6). Specifically, trimetazadine increased mitochondrial phospholipid turnover in rats that were treated trimetazadine over the course of 4 weeks. After treatment, treated and untreated rat myocytes were isolated and cultured for further phospholipid analysis. The results showed that the total amount of phospholipids in treated rats wasn't altered, but their qualitative composition was. The content of saturated fatty acids decreased while incorporation of unsaturated fatty acids increased in treated rats (6).

Based on these findings and on the knowledge we have about Barth syndrome, we think that with better understanding of the connection between the beta-oxidation pathway and mitochondrial phospholipid turnover, beta-oxidation inhibitors such as trimetazadine could possibly be used as a future treatment for Barth syndrome. This approach would target mitochondrial

phospholipid turnover to improve the underlying disease process, rather than just treating the already caused symptoms.

***S. cerevisiae* as a model organism**

Saccharomyces cerevisiae also known as Brewer's yeast, is a single-celled eukaryotic organism. Commonly used in the food industry for wine, bread and beer production due to its fermentation capabilities, *S. cerevisiae* has also proved to be an important model organism for studying and understanding eukaryote biology, as well as a wide range human diseases (8). What makes yeast practical for laboratory use is the fact that it is cheap and easier to work with than mammalian cells or animals in terms of storage and required growth conditions. Another advantage is using yeast for experiments can easily follow the reuse-reduce-recycle (3R) model and the absence of ethical boundaries. From the biology perspective, yeast cells have a high degree of conservation of many important cellular processes such as protein folding, translocation and secretion, autophagy, protein-protein interactions and energy metabolism. This makes them comparable to human cells, given the fact that 47% of essential yeast genes have a human ortholog (8). In this specific research, we are interested in thiolase enzymes. This enzyme family catalyses bond formation between carbon atoms and can be divided into two categories, based on whether they're involved in synthesis (e.g. steroid biogenesis, the mevalonate pathway) or degradation (e.g. the beta-oxidation pathway). Specifically, we are interested in the 3-ketoacyl-CoA mitochondrial thiolase involved in fatty acid degradation, which has its ortholog in *S. cerevisiae*, making it a great model organism for our study of how fatty acid degradation is connected to cardiolipin turnover.

Thesis objectives

Beta-oxidation is the pathway by which cells break down fatty acid molecules to generate acetyl-CoA for energy production (9). 3-ketoacyl coenzyme A thiolase is a key enzyme in the beta-oxidation pathway and the target of the partial fatty acid oxidation inhibitor, trimetazidine. One previous report indicated that treatment with trimetazidine is associated with increased mitochondrial phospholipid turnover, which may be beneficial in treating certain mitochondrial diseases like Barth syndrome (6). The yeast system is an ideal model system for studying how beta-oxidation influences mitochondrial phospholipid composition and turnover.

The main objectives of this thesis are:

- 1) Identify the yeast homolog of human 3-ketoacyl coenzyme A thiolase
- 2) Characterize the growth phenotypes of the yeast thiolase (POT1) knock out
- 3) Construct a *pot1Δtaz1Δ* yeast model

Materials and methods

Protein alignment

To confirm which gene in *Saccharomyces cerevisiae* encodes the protein that is most similar to the enzyme of our interest, the 3-ketoacyl-CoA thiolase (thiolase I) enzymes which are present in the beta-oxidation metabolic pathway, a protein sequence alignment of the human and yeast thiolase enzymes was performed using the DIOPT bioinformatic toolkit as previously described (10). The DIOPT bioinformatic toolkit allows for both protein and protein domain alignments, including percent amino acid identity, and is valuable for predicted ortholog pairs across species. Since it's previously known that *S. cerevisiae* has 2 genes that encode different thiolases, ERG10 and POT1 – to clarify which one is participating in synthesis and which one in degradation metabolic activities, both were compared to human genes that encode isoenzymes of the type I 3-ketoacyl-CoA thiolase (ACAA1, ACAA2, HADHB) and the type II acetoacetyl-CoA thiolase (ACAT1, ACAT2). Type I thiolase enzymes are associated with degradation pathways such as beta-oxidation while type II thiolase enzymes are responsible for biosynthesis paths such as steroid biogenesis.

***S. cerevisiae* cell lines**

The *pot1* Δ , *taz1* Δ and isogenic wild type (WT) control cell lines were graciously provided to us by prof. Miriam Greenberg from the Wayne State University in Detroit, Michigan, USA.

Growth conditions

All of our yeast strains were plated on yeast extract-peptone-dextrose (YPD) media and incubated at 30 °C. For each experiment, a single colony from the plates was used to start a liquid preculture which was then used to start cultures. The purpose of the preculture is to let the cells reach log phase when they are most competent and to allow us to start all cultures with the same number of cells – by measuring the optical density (OD) of precultures using a spectrophotometer and by calculating the volume of media that needs to be added to make a culture containing a specific number of cells. To find out after how many hours each strain is required to reach mid log phase, the OD of liquid cultures was measured at different timepoints (mostly every hour) so that a growth curve could be generated. Using the growth curve, the time each strain required to exit lag phase and enter log and stationary phases of growth was determined.

Glucose deprived spotting assay

Glucose deprivation was used to determine how the growth phenotype of *pot1Δ* cells compare to WT cells when forced to adapt to a lack of glucose by using alternative sources of carbon and energy (11). Firstly, the cells were precultured at 30 °C in 10 mL of synthetic minimal media that contains: yeast nitrogen base, glucose, minimal amino acid/base mix (uracil, histidine, leucine, methionine) and distilled water. When they entered log phase, they were cultured in the same media at the same OD value (in this case, 0.05 A_{600}). When the cultured cells reached mid log phase, they were centrifuged for 2 minutes at 3000 rpm and washed with synthetic minimal media without glucose. The now washed cells were again incubated at 30 °C but this time in 20 mL of synthetic minimal media lacking glucose. Every few days, the glucose deprived yeast were

spotted on to YPD plates and then incubated for 2 days to compare cell number after time of starvation and between WT and *pot1Δ*. The spotting was done by making a serial dilution which started at an OD of 0.5 A_{600} . Using a multichannel pipette, all 6 solutions (the first one having OD = 0.5, and the other 5 being serial dilutions of that one) were spotted on to the plates.

Fatty acid as sole carbon source spotting assay

To further determine the *pot1Δ* phenotype, another spotting assay was performed by using agar plates with oleic acid as the sole carbon source. Since fatty acids are broken down by beta-oxidation, cells with a beta-oxidation defect such as *pot1Δ*, would not be able to grow in media with fatty acids as the only carbon source. WT (control) and the *pot1Δ* mutant were cultured at 30°C in 10 mL of 0.3% glucose synthetic minimal media that contains: yeast nitrogen base, glucose, minimal amino acid/base mix (uracil, histidine, leucine, methionine) and distilled water. Typically SMD contains 2% glucose, but by lowering the glucose percentage, yeast cells would already start adapting to the low glucose conditions by altering their metabolism – increasing mitochondrial energy production instead of relying on glycolysis as the main pathway for obtaining energy. This way, the chances of control cells going into shock and not growing when transferred to oleic acid plates, is reduced. When the cells reached mid log phase, the liquid cultures were centrifuged for 3 minutes at 3500 rpm and washed 5 times with sterile distilled water, and their OD was adjusted to 0.5 (A_{600}). Afterwards, the cells were serially diluted into 5 solutions and spotted on to an synthetic minimal agar plate containing 0.1% oleic acid and 0.2% Tween-40 instead of glucose.

Extraction of genomic DNA from yeast

For the sake of confirming that *pot1Δ* mutant yeast cells lack the POT1 gene, genomic DNA was extracted from *pot1Δ* and WT yeast. One bigger colony of both strains was transferred from YPD plates to separate 1.5 mL tubes and suspended in 100 μL of 200 mM lithium acetate and 1% SDS solution. The inoculated solutions were then incubated for 5 minutes at 70 °C. After incubation, 300 μL of 100% ethanol was added and each tube was vortexed well. The DNA and cell debris were spined down at 15 000 g for 3 minutes, and the supernatant was discarded. The pellet was then washed with 70% ethanol and underwent centrifugation once more, after which all the supernatant was discarded by pipette. Samples were dried at 70 °C for 5 minutes with the tube lid open. When dry, 100 μL nuclease free water was added and the pellet was broken down by vortexing and resuspending until a cloudy suspension formed. The cell debris was centrifuged for 30 seconds at 15 000 g, and 2 μL of the supernatant was used for the upcoming PCR.

PCR and gel electrophoresis

The *pot1Δ* confirmation PCR was done using the forward 5'-tcttgaggctctgagtagagtgatataacactacataaaagccagctgaagcttcgtacgc-3' which has about 38% GC content. Because the 45bp right after the stop codon only has 20% GC an alternative nearby region was selected and reverse 5'-tgggccgcaatgcttcatttattcaaaaatatcgatatcttgggcataggccactagtgatctg-3' primer was constructed. The PCR reaction consisted of : 1 μL the 10 μM forward and reverse primer, a premade 2X mastermix that consisted of taq DNA polymerase, nucleotides and a buffer, 2 μL of the extracted genomic DNA and 6 μL of nuclease free water. The PCR program was as follows :

| | | | | |
|----|-------|------------|----------------------|-------------|
| 1. | 95 °C | 3 minutes | Initial denaturation | |
| 2. | 95 °C | 30 seconds | Denaturation | } 35 cycles |
| 3. | 55 °C | 30 seconds | Annealing | |
| 4. | 72 °C | 60 seconds | Extension | |
| 5. | 72 °C | 5 minutes | Final extension | |
| 6. | 12 °C | Held | | |

2 µl of each PCR product was added to wells in a 1% agarose gel containing 0.5 µl of a lab made gel dye. 4 µl of 6X Gel Star dye was added to each PCR product. A 100 bp DNA ladder (New England BIOLAB) was used for product length conformation. The loaded gel underwent electrophoresis for 45 minutes at 90V. After electrophoresis, the gel was examined under UV light to detect bands and determine the DNA size in bp.

Yeast transformation

To acquire *pot1Δtaz1Δ* double mutant yeast cells we attempted homologous recombination using a custom designed knock-out cassette. Since the *taz1Δ* yeast cells are lacking the gene for synthesizing uracil (selection marker) we designed a knock-out cassette, a linear DNA that contained the gene for uracil as well as sequences homologous to the part of the yeast genome where the *pot1* gene is located. That was done by designing primers using the *Saccharomyces* genome database to determine which base pairs are surrounding our gene of interest as well as the length of its coding region and its distance from other near genes of significance and by incorporating the knowledge we had of the sequence of our plasmid containing the uracil coding gene (pUG73). The forward primer used was 5'-tcttgaggctctgagtacagagtgaatataacactacataaaaagccagctgaagcttcgtacgc-3' and

the reverse primer was 5'-
 tgggccgcgaatgcttcatttatttcaaaaatatcgatatcttgggcataggccactagtggatctg-3' (the
 same primers used for the pot1Δ confirmation PCR. The PCR reaction
 consisted of : 0.5 μl of the pUG73 plasmid that was used as the DNA template,
 1 μl of both the forward and reverse primer (10 μM) previously designed to
 contain sequences homologous to both the plasmid and yeast DNA, 25 μl of
 the mastermix (2X) and finally 22.5 μl of nuclease free water, making up 50
 μl of content for the reaction. The PCR machine was programmed as follows :

| | | | | |
|----|-------|------------|----------------------|-------------|
| 1. | 95 °C | 1 minute | Initial denaturation | |
| 2. | 95 °C | 30 seconds | Denaturation | } 35 cycles |
| 3. | 79 °C | 30 seconds | Annealing | |
| 4. | 72 °C | 90 seconds | Extension | |
| 5. | 72 °C | 5 minutes | Final extension | |
| 6. | 4 °C | Held | | |

5 μl of the PCR product was combined with 1 μl of Gel Star dye (6X) to make
 a 1X solution which was then loaded on a 1% agarose gel together with a 100
 bp DNA ladder (New England BIOLAB). The loaded gel underwent
 electrophoresis for approx. 1 hour at 90V. After electrophoresis, the gel was
 examined under UV light to detect bands and determine the DNA size in bp.

After obtaining the DNA cassette which contained the gene for uracil and sequences homologous with the yeast POT1 gene, we attempted to transform *taz1Δ* and wild type yeast cells using the pUG73 plasmid, which would result in strains that lacked the POT1 gene and contained the URA3 gene. 2 different methods of yeast transformation were used on separate occasions: the one step yeast transformation (heat shock) method and electroporation.

One step yeast transformation

WT and *taz1Δ* yeast cells were cultured overnight in 10 mL of YPD media. The following day, 1 mL of WT and *taz1Δ* cells were transferred to a sterile microfuge tube and centrifuged for 5 minutes at 50% of the maximum speed. The supernatant was discarded, and the cells were suspended in 100 μ l of One step buffer. 1 mL of the One step buffer was prepared using 100 μ l of 2M lithium acetate, 666 μ l of 60% polyethyleneglycol, 100 μ l of freshly made 1M dithiothreitol and 134 μ l of distilled water. 1 mL of the buffer is enough for 10 transformations that use 1 mL of cells. After preparation, the buffer was filtered using a sterilization syringe filter (0.22 μ m). Prior to adding the PCR product, the buffer and cells mixture was held on ice. 10 μ l of the PCR product was then added to the mixture, vortexed and then incubated at 45 °C for 1 hour. 2 tubes (one containing *taz1Δ* and the other containing WT) were incubated without the uracil containing DNA as a negative control. After incubation, the cells were spread on plates containing uracil (control plates) and on plates lacking uracil to see whether the transformation was successful.

Electroporation

Same as for the one step yeast transformation, the transformation by electroporation was started by growing WT and *taz1Δ* cultures in 10 mL of YPD until their OD (measured by a spectrophotometer) was around 0.7 A_{600} . Cells were then centrifuged for 5 minutes at around 4500 g and resuspended in 10 mL of pretreatment buffer after which they were left to incubate at 30 °C for 30 minutes with gentle shaking. Unlike the one step buffer used in the previous transformation, the pretreatment buffer consists of 100mM lithium acetate, 10 mM TRIS, 1 mM EDTA, distilled water, 1M sucrose and freshly prepared 10 mM DTT. After incubation, the cells were washed 2 times with cold distilled water, and then 2 times with cold 1M sucrose while being kept on ice between and during each wash. The pellet was afterwards resuspended in 500 μ l of cold sucrose, mixed with 10 μ l of DNA and transferred to a cold electroporation cuvette. Since the program for yeast and bacteria wasn't working properly on the multiporator that was used for the experiment, we set the machine on mammalian program which pulsed the cells every 4 ms at 1.2 kV. Immediately after electroporating, 1 mL of YPD was added to the cells and they were left to recover for 1 hour at 30 °C. When recovered, the cells were once more centrifuged and resuspended in 100 μ l of cold sucrose and then plated on to uracil containing and uracil lacking plates.

Results

The overarching goal of this thesis is to develop a yeast model system for future use in interrogating the relationship between beta-oxidation and cardiolipin homeostasis. Inspired by previous reports that treatment with the beta-oxidation inhibitor, trimetazidine, results in increased phospholipid turnover, I first set out to verify which of the two yeast thiolase enzymes (POT1 and ERG10) is the homolog of the human 3-ketoacyl coenzyme A thiolase. Using the DIOPT bioinformatic toolkit (10) I first generated protein alignments. ACAA1, ACAA2, and HADHB are the three human Type I thiolase enzymes involved in beta-oxidation, and of these ACAA1 is the predominate isoform (12). As seen in figure 4, the protein alignment for ACAA1 and POT1 indicates the two proteins exhibit 51% conserved sequence identity. Figure 5 shows the protein alignment for ACAA1 and ERG10, which exhibit only 38% conserved sequence identity. Further analysis using the DIOPT bioinformatic toolkit indicate that the ACAA1 and POT1 have a homology score of 12/15, while ACAA1 and ERG10 have a homology score of 1/15.

Protein Alignment: ACAA1 and POT1

Sequence 1: NP_001598.1 **Gene:** ACAA1 **HGNCID:** 82 **Length:** 424 **Species:** Homo sapiens
Sequence 2: NP_012106.1 **Gene:** POT1 **SGDID:** S000001422 **Length:** 417 **Species:** Saccharomyces cerevisiae

Alignment Length: 431 **Identity:** 220/432 (51%)
Similarity: 273/432 (63%) **Gaps:** 32/432 (7%)

```

Human 2 QRLQVVLGHL-RGFADSGWMPQAPCLSGAPQASAADVVVHGRRTAICRAGRGGFKDTPDELL 65
      | | | | : . . | | . . . . . | . . . . . | . . . . . | | | | : | . . . | | : . . . . | | | | . . | |
Yeast 3 QRLQSIKDHLVESAMGKGESKRKNSLLEKRPE---DVVIVAANRSAIGKGFKAQFVNDYLL 63
      | | | | : . . | | . . . . . | . . . . . | . . . . . | | | | : | . . . | | : . . . . | | | | . . | |
Human 66 SAVMTAVL-----KDVNLRPEQLGDIQVGNVLQPGAGAIMARIAQFLSDIPETVPLSTVNRQ 122
      . . . . . : | : | | : . . . . . | | | | | . . . . . | | | | | . . . . . | | | | | . . . . . | |
Yeast 64 YNFLNEFIGRFPEELRADLNL---IEEVACGNVNLVAGAGATEHRAACLASGIPISTPFVVALNRQ 124
      | | | | : . . | | . . . . . | . . . . . | . . . . . | | | | : | . . . | | : . . . . | | | | . . | |
Human 123 CSSGLQAVASIAAGGIRNGSYDIGMACGVESMSLADRG-NF-GNITSRLMEKEK-ARDCLIPMGIT 184
      | | | | . | | . | | . . | | : | | | | | . . . . . | | | | | . . . . . | | | | | . . . . . | |
Yeast 125 CSSGLTAVNDIANKIKVQIDIGLALGVESMTNNYKNWNPLGMISSEELQKNREAKKCLIPMGIT 189
      | | | | . | | . | | . . | | : | | | | | . . . . . | | | | | . . . . . | | | | | . . . . . | |
Human 185 SENVAERFGISREKQDTFALASQQKAARAQSKGCFQAEIVPVTITVHDDKGTKRISITVTQDEGIR 249
      : | | | . . | | : . . | | . . | | . . | | : | | : | | : | | : | | : | | : | | : | | : | | : | |
Yeast 190 NENVAANFKISRKQDEFAANSYQKAYKARNEGLFEDEILPI-----KLPDGI-CQSDEGPR 246
      | | | | : . . | | . . . . . | . . . . . | . . . . . | | | | : | . . . | | : . . . . | | | | . . | |
Human 250 PSTMEGLAKLKPAPFKD-GSTTAGNSSQVSDGAAAILLARRSKAEELGLPILGVLSYAVVGV 313
      | : | . | | : : : | | | | | | | | | | | | | | | | | | | | | | | | | | | | | | | | | | | | | | | | |
Yeast 247 PNVTAESLSSIRPAFIKDRGTTTAGNASQVSDGVAGVLLARRSVANQLNLVPLGRYIDFQTVGV 311
      | : | . | | : : : | | | | | | | | | | | | | | | | | | | | | | | | | | | | | | | | | | | | | | | | |
Human 314 PDIMGIGPAYAIPVALQKAGLTVSDVDIFEINEAFASQAAYCVEKLRPLPEKVNPLGGAVALGHP 378
      | : | | | | | | | | | | | | | | | | | | | | | | | | | | | | | | | | | | | | | | | | | | | | | | |
Yeast 312 PEIMGVGPAYAIPKVLQGLVQDIDIFEINEAFQAALYCIHKLGLDNLKVNPRGGAIALGHP 376
      | : | | | | | | | | | | | | | | | | | | | | | | | | | | | | | | | | | | | | | | | | | | | | | | |
Human 379 LGCTGARQVITLNLKRRGKRAYGVVSMCIQGTGMGAAAVF 419
      | | | | | | | | | | | | | | | | | | | | | | | | | | | | | | | | | | | | | | | | | | | | | | |
Yeast 377 LGCTGARQVATILRELK---KDQIGVVSMCIQGTGMGAAAVF 414
      | | | | | | | | | | | | | | | | | | | | | | | | | | | | | | | | | | | | | | | | | | | | | | |
    
```

Figure 4 : Protein alignment of human ACAA1 and yeast POT1 gene. Gene length and order of amino acids coded by ACAA1 and POT1 genes were compared and checked for identity and similarity, with ACAA1 coding human 3-Ketoacyl-CoA thiolase (thiolase type I) and POT1 coding the yeast thiolase (thiolase type I). Each letter presents one amino acid. Straight lines between letters (amino acids) indicate identity, dots indicate similarity and dashes show gaps between sequences. The alignment was generated using FlyBase.

homology score of 12/15, while ACAT1 and POT1 have a homology score of 2/15.

Protein Alignment: ACAT1 and ERG10

Sequence 1: NP_000010.1 Gene: ACAT1 HGNCID: 93 Length: 427 Species: Homo sapiens
Sequence 2: NP_015297.1 Gene: ERG10 SGDID: S000005949 Length: 398 Species: Saccharomyces cerevisiae

Alignment Length: 400 Identity: 196/400 (49%)
Similarity: 266/400 (67%) Gaps: 16/400 (4%)

```
Human 40 KEVVIVSATRTPIGSFLGSLSLLPATKLGSIAIQGAIEKAGIPK---EEVKEAYMGNVLQGGEG 100
      :|.|||||.|||||.|||||.|||:|:|:|:|:|:|  :|:  :|...|...|...|...|
Yeast 3 QNVYIVSTARTPIGSFQGSLSKKTAVELGAVALKGALAK--VPELDASKDFDEIIFGNVLSANLG 65
Human 101 QAPTRQAVLGAGLPITPCTTINKVCASGMKAIMMASQSLMCGHQDVMVAGGMESMSNVPYVM-- 163
      |||.|||.|||.|||.|||.|||.|||.|||.|||.|||.|||.|||.|||.|||.|||.|||.|||.
Yeast 66 QAPARQVALAAGLSNHIVASTVNKVCASAMKAIILGAQSIKCGNADVVVAGGCESMTNAPYYMFA 130
Human 164 NRGSTPYGGVKLEDLIVKDGLTDVYNKIHMGSCAENTAKKLNARNEQDAYAINS YTRSKAAWEA 228
      .|...:|...|.||:|||||.||:|...||...||...:|...|...|...|...|...|...|...
Yeast 131 ARAGAKFGQTVLVDGVERDGLNDAYDGLAMGVHAEKCARDWDITREQQDNFAIESYQKSQKSQKE 195
Human 229 GKFGNEVIPVTVT-VKGGPDVVVKEDEEYKRVDFSKVPKLKTVPKQKENGTVTAANASTLNDGAAA 292
      |||.||:|...  :|:|...|...|...|...|...|...|...|...|...|...|...|...|...
Yeast 196 GKFDNEIVPVTIKGFRGKPDVTQVKDEEPARLHVEKLRSAITVFQKENGTVTAANASPFINDGAAA 260
Human 293 LVLMTADAAKRLNVTPLARIVAFADA AVEPIDFPIAPVYAASMLKDVGLKEDI---AMWEVNE 354
      :|:|...|...|...|...|...|...|...|...|...|...|...|...|...|...|...|...
Yeast 261 VILVSEKVLKEKNLKLPLAIKGWGEAAHQPADFTWAPSLAVPKALKHAGI--EDINSVDYEFENE 323
Human 355 AFSLVVLANIKMLEIDPQKVNINGGAVSLGHPIGMSGARIVGHLTHALKQ--GEYGLASICNGGG 417
      |||:|.|||.||:|...|...|...|...|...|...|...|...|...|...|...|...|...|...
Yeast 324 AFSVVGLVNTKILKLDPSKVN VYGGAVALGHPLGCSGARVVVTLLSILQQEGGKIGVA AICNGGG 388
Human 418 GASAMLIQKL 427
      |||:|...|...
Yeast 389 GASSIVIEKI 398
```

Figure 6 : Protein alignment of human ACAT1 and yeast ERG10 gene. Gene length and order of amino acids coded by ACAT1 and ERG10 genes were compared and checked for identity and similarity, with ACAT1 coding human acetoacetyl-CoA thiolase (thiolase type II) and ERG10 coding the yeast thiolase (thiolase type II). Each letter presents one amino acid. Straight lines between letters (amino acids) indicate identity, dots indicate similarity and dashes show gaps between sequences. The alignment was generated using FlyBase.

Protein Alignment: ACAT1 and POT1

Sequence 1: NP_000010.1 **Gene:** ACAT1 **HGNCID:** 93 **Length:** 427 **Species:** Homo sapiens
Sequence 2: NP_012106.1 **Gene:** POT1 **SGDID:** S000001422 **Length:** 417 **Species:** Saccharomyces cerevisiae

Alignment Length: 401 **Identity:** 136/402 (34%)
Similarity: 208/402 (52%) **Gaps:** 31/402 (8%)

```

Human   40 KEVVIVSATRTPIG-SFLGSLLLPATKLGSIATQGAIEKAGIPKEE----VKEAYMGNVLQGGE  99
      ::|||::|.|:| | .|.|:.....|.....|.....|.....|.....|.....|.....|.....
Yeast   34 EDVVIVAANRSAIGKGFKGFKDVNTDYLLYNFLNEFIGRFPEPLRADLNLIIEVACGNVLNVGA  98
Human  100 GQAPTRQAVLQAGLPITPCTTINKVCASGMKAIMMASQSLMCGHQDVMVAGGMESMSNVPYVM  164
      |...|.|.|:|:|:|:|:|:|:|:|:|:|:|:|:|:|:|:|:|:|:|:|:|:|:|:|:|:|:|:|:|:|:|
Yeast   99 GATEHRAACLASGIPYSTPFVALNRQCSSGLTAVNDIANKIKVQGQIDIGLALGVESMTN----NY  159
Human  165 RGSTPYGGVKLEDLIVKDGLTDVYNK-----IHMGSCAENTAKKLNARNEQDAYAINSYTRSK  223
      :...|.|.|:|:|:|:|:|:|:|:|:|:|:|:|:|:|:|:|:|:|:|:|:|:|:|:|:|:|:|:|:|:|
Yeast  160 KNVNPLGMISSSEEL-----QKNREAKKCLIPMGITNENVAANFKISRKQDEFANASYQKAY  216
Human  224 AAWEAGKFGNEVIPVTIVTKGQPDVVVKEDEEYKR--VDFSKVPKTKTVFKENGTVTAANASTL  286
      .|...|.|.|:|:|:|:|:|:|:|:|:|:|:|:|:|:|:|:|:|:|:|:|:|:|:|:|:|:|:|:|
Yeast  217 KAKNEGLFEDEILPIKL-----PDGSICQSDEGPRPNVTAESLSSIRPAFIKDRGTTAGNASQV  276
Human  287 NDGAAALVMTADAARKRLNVTPLARIVAFADAAVEPIDFPFIAPVYAASVMVKDVLKEDIAMWE  351
      :||:|:|:|:|:|:|:|:|:|:|:|:|:|:|:|:|:|:|:|:|:|:|:|:|:|:|:|:|:|:|:|
Yeast  277 SDGVAGVLLARRSVANQLNLPVLGRYIDFQTVGVPPEIMGVGPAYAI PKVLEATGLQVQDIDIFE  341
Human  352 VNEAFSLVLANIKMLEIDPQKVNINGGAVSLGHPIGMSGARIVGHLLTHALKQGEYGLASICNGG  416
      :|||:....|.|.|:|:|:|:|:|:|:|:|:|:|:|:|:|:|:|:|:|:|:|:|:|:|:|:|:|:|:|
Yeast  342 INEAFAAQALYCIHKLGIDLNKVNPRGGATALGHPLGCTGARQVATILRELKQDIGVVMSCIGT  406
Human  417 G-GASAMLIQK 426
      | ||:|.|:|:|
Yeast  407 GMGAAAFIPE 417
  
```

Figure 7 : Protein alignment of human ACAT1 and yeast POT1 gene. Gene length and order of amino acids coded by ACAT1 and POT1 genes were compared and checked for identity and similarity, with ACAT1 coding human acetoacetyl-CoA thiolase (thiolase type II) POT1 coding the yeast thiolase (thiolase type I). Each letter presents one amino acid. Straight lines between letters (amino acids) indicate identity, dots indicate similarity and dashes show gaps between sequences. The alignment was generated using FlyBase.

Given that the DIOPT bioinformatic analysis confirmed POT1 to be the yeast homolog of the human 3-Ketoacyl-CoA thiolase, the next step in this thesis was to confirm that the *pot1Δ* mutant yeast was indeed lacking the POT1 gene by PCR, with WT as the control. Figure 8 depicts the PCR results of WT and *pot1Δ*.

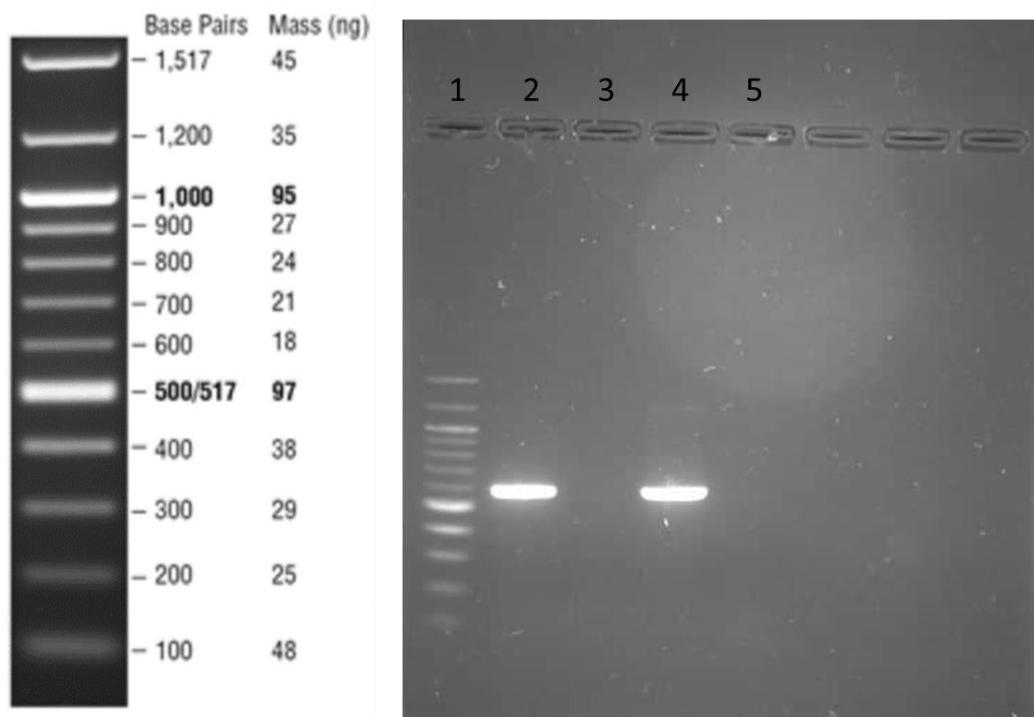


Figure 8 : PCR conformation of *pot1Δ*. A 100 bp DNA ladder (New England BIOLAB) was loaded in well number 1. Wells number 2 and 4 were loaded with WT DNA and wells number 3 and 5 with *pot1Δ* DNA. Since primers for the POT1 gene were used in this PCR, the expected result was that WT DNA would show bands if the POT1 gene was replicated successfully, given the fact that WT yeast contain the POT1 gene and use as a control in this assay. The other expected result was that *pot1Δ* DNA would not show any bands if the POT1 gene is missing. Knowing that the length of the POT1 gene is 600 bp, the bands of WT DNA would be the same length. Since all of the expected results were obtained, this confirms that the *pot1Δ* mutant indeed lacks the POT1 gene.

I next sought to see how the growth of the *pot1Δ* strain compared to WT using standard yeast culturing techniques. As seen in Figure 9, when grown with glucose as the carbon source *pot1Δ* grows similarly as WT with no apparent reduction in growth.

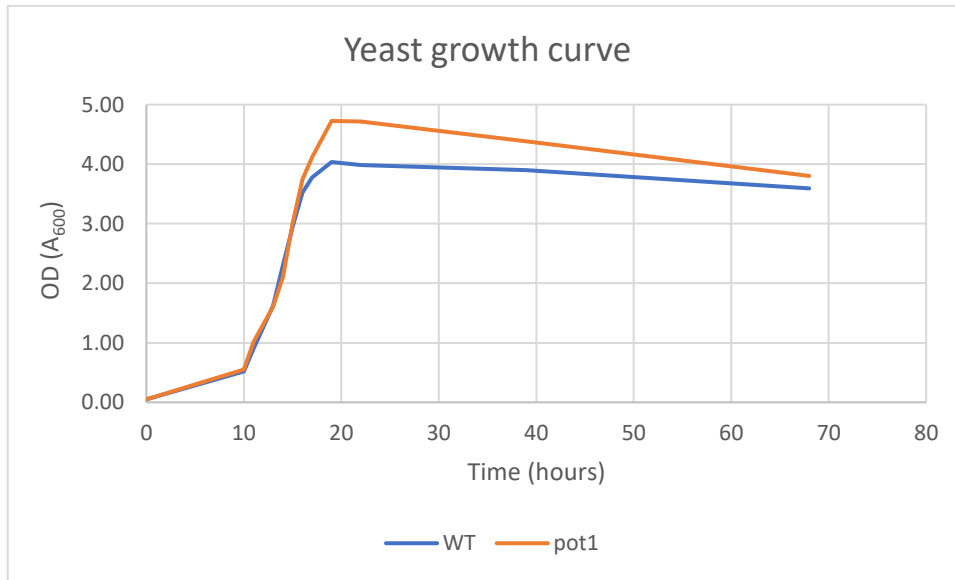


Figure 9 : Yeast growth curve. Cultures of WT and *pot1Δ* started at OD = 0.05 in synthetic minimal media were grown at 30°C. Using a spectrophotometer, their OD was measured during time – more frequently during the first 24 hours and less often over the course of the next 3 days. The measured OD values are proportional to the number of cells present in the cultures at different time points. Rapid growth of cells shown by the part of lines which are similar to those of an exponential function indicate the time point of cells exiting lag and entering log phase, while the decrease in cell number shown by the lines becoming linear indicates cells entering lag phase.

Because beta oxidation is important for survival of yeast cells during glucose starvation, I next sought to determine how the *pot1Δ* strain grows compared to WT when exposed to glucose starvation. Figure 10 shows a typical spotting assay of *pot1Δ* and WT at different timepoints during the glucose starvation.

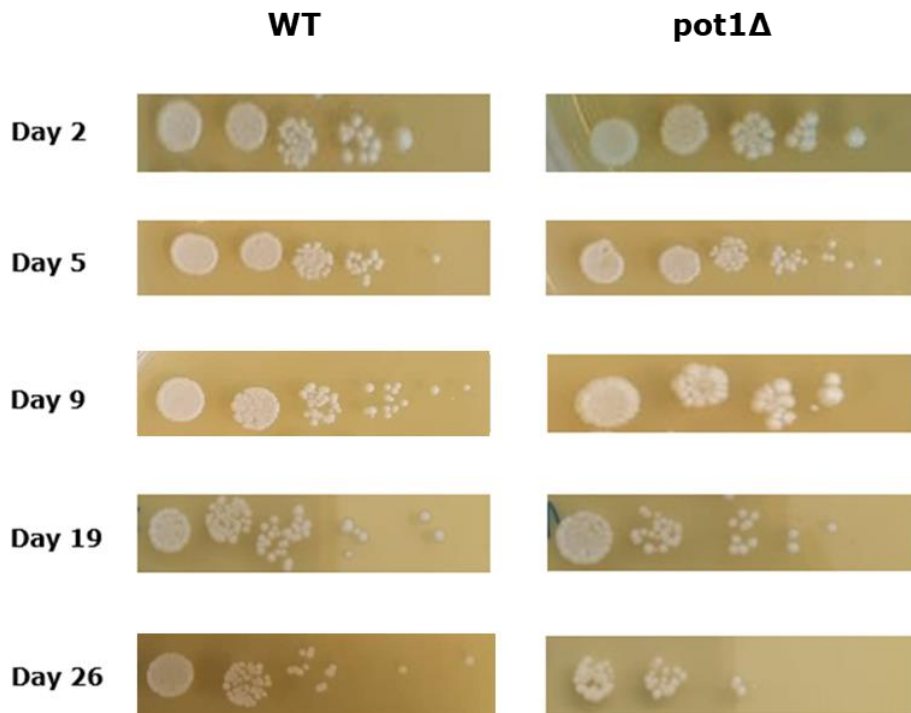


Figure 10 : Glucose starvation spotting assay of yeast mutants WT and *pot1Δ*. Cultures of WT and *pot1Δ* grown in Synthetic minimal media without glucose were serially diluted and spotted on to YPD plates over the course of 26 days. Each spot contains 2 μ L of culture solution, the first spot being diluted 4 times (1:3), and every other spot being diluted 5 times (1:4) more than the previous spot.

Another method used for comparing growth phenotypes between WT and *pot1Δ* was growing them on oleic acid plates. Figure 11 shows that *pot1Δ* is unable to grow on media in which beta-oxidation is the only metabolic

pathway available for obtaining energy, due to the lack of 3-ketoacyl-CoA thiolase.



Figure 11 : Spotting assay using fatty acids as the sole carbon source. Cultures of WT and *pot1Δ* grown in 0.3% glucose synthetic minimal media were serially diluted and spotted on to 0.2% oleic acid plates after 10 days of cultivation. Each spot contains 2 μ L of culture solution, the first spot being diluted 4 times (1:3), and every other spot being diluted 5 times (1:4) more than the previous spot.

To generate the desired *pot1Δtaz1Δ* double mutant yeast, I next constructed a knock out cassette which would allow me to knock out the POT1 gene from *taz1Δ* mutant yeast by homologous recombination (14). The cassette was constructed using excision primers for the POT1 gene, as well as primers homologous to the pUG73 plasmid. Afterwards, the cassette was multiplied by PCR.

Figure 12 depicts the PCR result, and confirms that the generation of the knock out cassette was successful; the length of the DNA is around 1700 bp, which is the length previously described in literature (14)

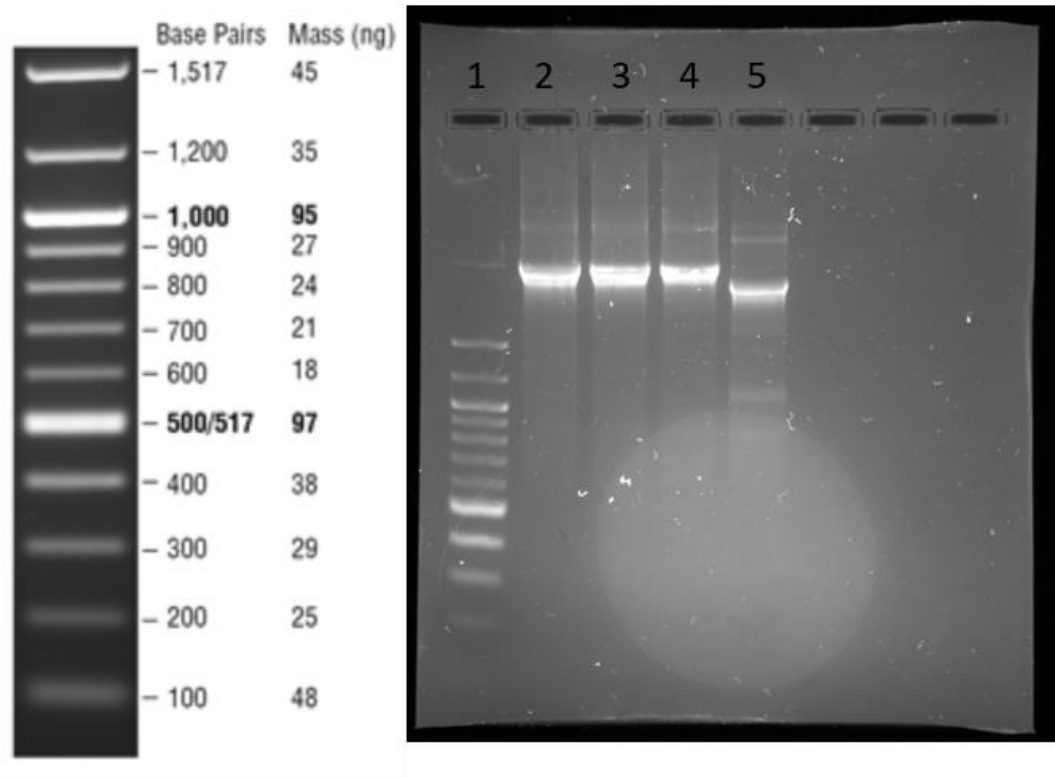


Figure 12 : Generation of the knock out cassette by PCR. A 100 – 1 517 bp DNA ladder (New England BIOLAB) was loaded in well number 1. Our PCR product, DNA containing a gene for uracil and sequences homologous to the yeast base pairs near the POT1 gene, was loaded in wells number 2, 3 and 4. Well number 5 was loaded with another PCR product containing DNA that had a gene for leucine. Given the fact that it is known that the uracil containing DNA should be around 1.7 kbp in size, and the leucine containing one around 2.5 kbp (14)the bands were compared to the 100 – 1 517 bp DNA ladder.

Discussion

By analyzing the protein alignments, we confirmed that *S. cerevisiae* has both synthesis and degradation thiolases, making it a fitting model organism for studying metabolic pathways in which thiolase enzymes are involved, such as beta-oxidation. Based on the identity and similarity percentage between yeast and human genes, we determined that acetyl-coenzyme A acetyltransferase (thiolase type II) is present in yeast cells and coded by ERG10, while 3-ketoacyl-CoA thiolase (thiolase I) is also present in yeast and coded by POT1. These findings are consistent with previous functional studies of yeast lacking POT1 (15,16). The identity between POT1 and human genes coding isoenzymes of thiolase I is above 30%, with a similarity above 40%. The same follows for ERG10 and genes coding isoenzymes of thiolase II with only slightly higher percentages (1-5% higher similarity and identity than POT1).

Given the fact that *pot1Δ* lacks the 3-ketoacyl-CoA thiolase (thiolase I) enzyme, it should not be able to use its mitochondria for obtaining energy by the beta-oxidation pathway. We compared *pot1Δ* to WT in 2 conditions where beta-oxidation was required: during a 26 day glucose starvation assay, and by cultivation on plates that contain only oleic acid as a carbon source. Our expectations from the glucose starvation assay were that *pot1Δ* should show a bigger decrease in cell number over time. As expected, after 19 days of glucose starvation we can clearly see that *pot1Δ* is growing less compared to WT, proving its phenotype – because of the absence of 3-ketoacyl-CoA thiolase, *pot1Δ* can't break down fatty acids by beta-oxidation, which makes generating energy without glucose even harder. Regarding the assay in which WT and *pot1Δ* were grown on oleic acid, we expected that it would take more than a week for both strains to grow (17) and that *pot1Δ* won't grow on this media at all, while WT would grow, but significantly less and slower compared to its growth on glucose containing media. Our results show that *pot1Δ* did manage

to grow, but significantly less than WT. The reasons why *pot1Δ* did manage to grow in these conditions may be inadequate washing of the 0.3% glucose SMD media in which it was cultured before spotting and possible traces of glucose in the oleic acid plates.

Since the goal was to make our own *pot1Δ* and *pot1Δtaz1Δ* by knocking out POT1 gene from WT and *taz1Δ* yeast, many copies of DNA that contains the gene for uracil as well as homologue sequences to the yeast genome were made by PCR from the Pug72 plasmid. The reason why we wanted to knock out POT1 from WT was to make sure that we have cells lacking POT1 specifically. We also wanted to see if the lack of POT1 in *taz1Δ* would rescue its growth or improve its cardiolipin profile. The PCR was successful, as the size of our DNA was confirmed to be around 1.7 kbp. The cells that we were working with were lacking not only the gene for uracil but also for leucine, so a PCR with the Pug73 plasmid containing leucine was also done. This PCR was unsuccessful, as our PCR product is the size of around 1.8 kbp while it should be the size of 2.5 kbp (8). The probable reason for this reaction not working is the PCR program that we used – since this DNA is so big in size, time of denaturation, annealing and extension should have been longer than 30 seconds.

To knock out POT1 from WT and *taz1Δ*, we attempted 2 methods of yeast transformation. When our PCR product, DNA containing sequences homologue to the yeast DNA surrounding POT1 would enter the cell, it would insert the gene for uracil and knock out POT1 by homologous recombination. Afterwards, the cells that successfully underwent transformation would be able to grow on media without uracil as they would be able to synthesize it themselves. Neither of our transformations worked, with no single colonies showing on URA-plates. There are multiple reasons why this happened, first being the size and structure of the inserted DNA. Another reason is the process of homologous

recombination, which is a random process that doesn't occur at all times and can hardly be affected with other methods and procedures.

The electroporation method has more promise in being successful compared to the one step yeast transformation method, but since our multiporator didn't work on the "yeast and bacterial" setting, we were forced to use the "mammalian" setting which pulses the cells at a lower voltage. Mammalian cells don't have a cell wall, which means the lower voltage might have not been enough to pierce through both the yeast cell wall and cell membrane.

Future goals and objectives

Other experiments and data we would like to collect regarding how beta-oxidation influences mitochondrial phospholipid turnover include a successful generation of the *pot1Δtaz1Δ* mutant using sporulation rather than relying on homologous recombination via electroporation or the heat shock method. Sporulation is a molecular mechanism that is the yeast's way of responding to nutrient deprivation which leads cells to exit the mitotic cell cycle and enter into meiosis, leading to spore formation (18). This way, the *pot1Δtaz1Δ* mutant can be generated from its parent *taz1Δ* and *pot1Δ* cells, and it can be confirmed by PCR and by growth on plates lacking an amino acid (eg. leucine) or nitrogen base (e.g. uracil), depending on which genes the parent cells are lacking and WT isn't. Another objective is to quantify the cardiolipin from *taz1Δ*, *pot1Δ*, *pot1Δtaz1Δ* and WT and its structural differences between strains, using mass spectrometry. The final goal after the previously mentioned two objectives are reached, would be to treat the *pot1Δtaz1Δpot1Δ* with trimetazidine, and compare their cardiolipin and mitochondrial function to untreated cells.

Conclusion

With genetic diseases being incurable, it should be in our best interest to not only treat their symptoms, but to understand their molecular mechanisms to find new drug targets and treatment approaches that could possibly allow patients to live longer more normal lives. Barth syndrome, although compromising only one cell organelle, the mitochondria, comes with a wide range of comorbidities, most of them focusing on the heart and skeletal muscles. Because of this, symptomatic treatment is very difficult – it takes a variety of different medication to cover all the malfunctioning organs and to narrow down symptoms, causing even more health issues. This is the main reason why we should focus on finding out why is the cardiolipin remodeling pathway so important, what are its roles in the mitochondria, and how can it be influenced by other, preferably existing substances. Trimetazadine has shown potential in mitochondrial phospholipid turnover, and could be a drug of choice if we find understanding in the importance of the TAZ1 gene and its functions. *Saccharomyces cerevisiae* is a widely used model organism because of being a sustainable and reliant eukaryotic organism with many genetic similarities to humans. It is a perfect tool for studying Barth syndrome because it can efficiently mimic the disease and allow further analysis of its molecular mechanism, as well as testing new treatment targets. Since the mitochondrial phospholipid cardiolipin is the main molecular alteration caused by Barth syndrome, a new treatment approach could be targeting beta-oxidation, which would allow more phospholipid precursors to be available to the cell, possibly altering mitochondrial phospholipid constitution, resulting in reduced MLCL intermediate accumulation and thus enhancing mitochondrial function in Barth syndrome.

References

1. Clarke SL, Bowron A, Gonzalez IL, Groves SJ, Newbury-Ecob R, Clayton N, et al. Barth syndrome [Internet]. Vol. 8, Orphanet Journal of Rare Diseases. 2013. Available from: <http://www.orphandb.com/content/8/1/23>
2. Ferreira C, Pierre G, Thompson R, Vernon H. Barth Syndrome. 1993.
3. Chin MT, Conway SJ. Role of Tafazzin in Mitochondrial Function, Development and Disease. *J Dev Biol*. 2020 May 23;8(2):10.
4. Ye C, Lou W, Li Y, Chatzisprou IA, Hüttemann M, Lee I, et al. Deletion of the Cardiolipin-specific Phospholipase Cld1 rescues growth and life span defects in the Tafazzin Mutant implications for Barth Syndrome. *Journal of Biological Chemistry*. 2014 Feb 7;289(6):3114–25.
5. Bertero E, Kutschka I, Maack C, Dudek J. Cardiolipin remodeling in Barth syndrome and other hereditary cardiomyopathies. Vol. 1866, *Biochimica et Biophysica Acta - Molecular Basis of Disease*. Elsevier B.V.; 2020.
6. Sentex E, Sergiel JP, Lucien A, Grynberg A. Trimetazidine increases phospholipid turnover in ventricular myocyte. Vol. 175, *Molecular and Cellular Biochemistry*. 1997.
7. Ezsi CAD. Trimetazidine in Practice: Review of the Clinical and Experimental Evidence [Internet]. 2015. Available from: www.americantherapeutics.com
8. Nielsen J. *Yeast Systems Biology: Model Organism and Cell Factory*. Vol. 14, *Biotechnology Journal*. Wiley-VCH Verlag; 2019.
9. Houten SM, Wanders RJA. A general introduction to the biochemistry of mitochondrial fatty acid β -oxidation. Vol. 33, *Journal of Inherited Metabolic Disease*. 2010.
10. Hu Y, Flockhart I, Vinayagam A, Bergwitz C, Berger B, Perrimon N, et al. An integrative approach to ortholog prediction for disease-focused and other functional studies. *BMC Bioinformatics*. 2011;12.
11. Weber CA, Sekar K, Tang JH, Warmer P, Sauer U, Weis K. β -Oxidation and autophagy are critical energy providers during acute glucose depletion in *Saccharomyces cerevisiae*. *Proc Natl Acad Sci U S A*. 2020;117(22).
12. Bout A, Hoovers J, Bakker E, Mannens MMAM, van Geurts Kessel A, Westerveld A, et al. Assignment of the gene coding for human peroxisomal 3-oxoacyl-coa thiolase (ACAA) to chromosome region 3p22→p23. *Cytogenet Genome Res*. 1989;52(3–4).
13. Long T, Sun Y, Hassan A, Qi X, Li X. Structure of nevanimibe-bound tetrameric human ACAT1. *Nature*. 2020;581(7808).
14. Hegemann JH, Gldener U, Köhler GJ. Gene disruption in the budding yeast *Saccharomyces cerevisiae*. *Methods Mol Biol*. 2006;313.

15. Erdmann R. The peroxisomal targeting signal of 3-oxoacyl-coA thiolase from *Saccharomyces cerevisiae*. *Yeast*. 1994;10(7).
16. Igual JC, Matallana E, Gonzalez-Bosch C, Franco L, Pérez-Ortín JE. A new glucose-repressible gene identified from the analysis of chromatin structure in deletion mutants of yeast *SUC2* locus. *Yeast*. 1991;7(4).
17. van Roermund CWT, Waterham HR, Ijlst L, Wanders RJA. Fatty acid metabolism in *Saccharomyces cerevisiae*. Vol. 60, *Cellular and Molecular Life Sciences*. 2003. p. 1838–51.
18. Tomar P, Bhatia A, Ramdas S, Diao L, Bhanot G, Sinha H. Sporulation Genes Associated with Sporulation Efficiency in Natural Isolates of Yeast. *PLoS One*. 2013;8(7).

List of figures

| | |
|--|----|
| Figure 1 : Barth syndrome indications..... | 2 |
| Figure 2 : Cardiolipin synthesis and remodeling in <i>S. cerevisiae</i> | 3 |
| Figure 3 : Deletion of CLD1 rescues growth in <i>taz1Δ</i> yeast mutant..... | 4 |
| Figure 4 : Protein alignment of human ACAA1 and yeast POT1 gene..... | 17 |
| Figure 5 : Protein alignment of human ACAA1 and yeast ERG10 gene..... | 18 |
| Figure 6 : Protein alignment of human ACAT1 and yeast ERG10 gene..... | 19 |
| Figure 7 : Protein alignment of human ACAT1 and yeast POT1 gene..... | 20 |
| Figure 8 : PCR conformation of <i>pot1Δ</i> | 21 |
| Figure 9 : Yeast growth curve..... | 22 |
| Figure 10 : Glucose starvation spotting assay of yeast mutants WT and <i>pot1Δ</i> | 23 |
| Figure 11 : Spotting assay using fatty acids as the sole carbon source..... | 24 |
| Figure 12 : Generation of the knock out cassette by PCR..... | 25 |